JMEPEG (2012) 21:1744–1750
DOI: 10.1007/s11665-011-0070-6

1059-9495/$19.00

Microstructure, Morphology, and Nanomechanical Properties Near Fine Holes Produced by Electro-Discharge Machining

P.J. Blau, J.Y. Howe, D.W. Coffey, R.M. Trejo, E.D. Kenik, B.C. Jolly, and N. Yang

(Submitted August 3, 2011)

Fine holes in metal alloys are employed for many important technological purposes, including cooling and the precise atomization of liquids. For example, they play an important role in the metering and delivery of fuel to the combustion chambers in energy-efficient, low-emission diesel engines. Electro-discharge machining (EDM) is one process employed to produce such holes. Since the hole shape and bore morphology can affect fluid flow, and holes also represent structural discontinuities in the tips of the spray nozzles, it is important to understand the microstructures adjacent to these holes, the features of the hole walls, and the nanomechanical properties of the material that was in some manner altered by the EDM hole-making process. Several techniques were used to characterize the structure and properties of spray-holes in a commercial injector nozzle. These include scanning electron microscopy, cross sectioning and metallographic etching, bore surface roughness measurements by optical interferometry, scanning electron microscopy, and transmission electron microscopy of recast EDM layers extracted with the help of a focused ion beam.

Keywords automotive, carbon/alloy steels, metallography

1. Introduction

Fine holes in metal alloys are employed for many important technological purposes, including cooling and the precise atomization of liquids. They play a particularly important role in fuel injection systems in heavy vehicle and other diesel engines because they can affect not only the combustion timing and fuel efficiency, but also the exhaust gas emissions. Over the past 30 or more years, there has been a trend to raise the operating pressure in fuel injectors. These higher pressures increase spray penetration into the combustion chamber and promote better fuel burning characteristics (Ref 1); however, higher operating pressures also places additional demands on the alloys of which the nozzles are composed. In fact, injector pressures in excess of 2000 bars (200 MPa or 29,000 psi) are planned for the next generation of fuel efficient diesel engines.

Electro-discharge machining (EDM) is widely employed to produce small, 50-300 μm diameter holes in fuel injector tips, called "sacks." The enormous number of holes to be produced quickly, and with tolerances of 2 μm or less, has led to the development of highly automated EDM hole-making technologies (e.g., Ref 2). While the shape and bore morphology of holes affect air-fuel mixture flow, the holes can, in principle, form localized stress concentrations to initiate fatigue cracks. As the high pressures place additional demands on nozzle materials it becomes increasingly important to understand the microstructures adjacent to the spray holes, the features of the hole walls, and the nanomechanical properties of the material that has been altered by the EDM hole-making process. These characterizations were the focus of this investigation.

P.J. Blau, J.Y. Howe, D.W. Coffey, R.M. Trejo, E.D. Kenik, and **B.C. Jolly**, Materials Science and Technology Division, Oak Ridge National Laboratory, Oak Ridge, TN 37831; **N. Yang**, Caterpillar Inc., Peoria, IL. Contact e-mail: blaupj@ornl.gov.

2. Experimental Methods and Results

Several complementary methods were employed to characterize the holes and near-hole materials in a commercially produced, alloy steel nozzle from a production heavy vehicle diesel engine. The material was a heat-treated alloy steel, and representative parts are shown in Fig. 1. Initial studies included cross sectioning, etching, and microindentation hardness profiling of nozzles in the sack area to determine whether there were any gradients in mechanical properties through the thickness of the bulk material in which the holes had been formed. Subsequently, precision machining methods were used to produce axial cross sections of individual holes for scanning electron microscopy (SEM) and measurement of the surface roughness parameters and profiles of the hole bore. Further cross sectioning enabled nanoindentation hardness measurements of EDM recast layers. Finally, a focused ion beam (FIB) method enabled slices to be removed from the recast-layer to study the manner in which the fine structure of the alloy steel had been altered by the hole-making process. The methods used and results of the examination follow.

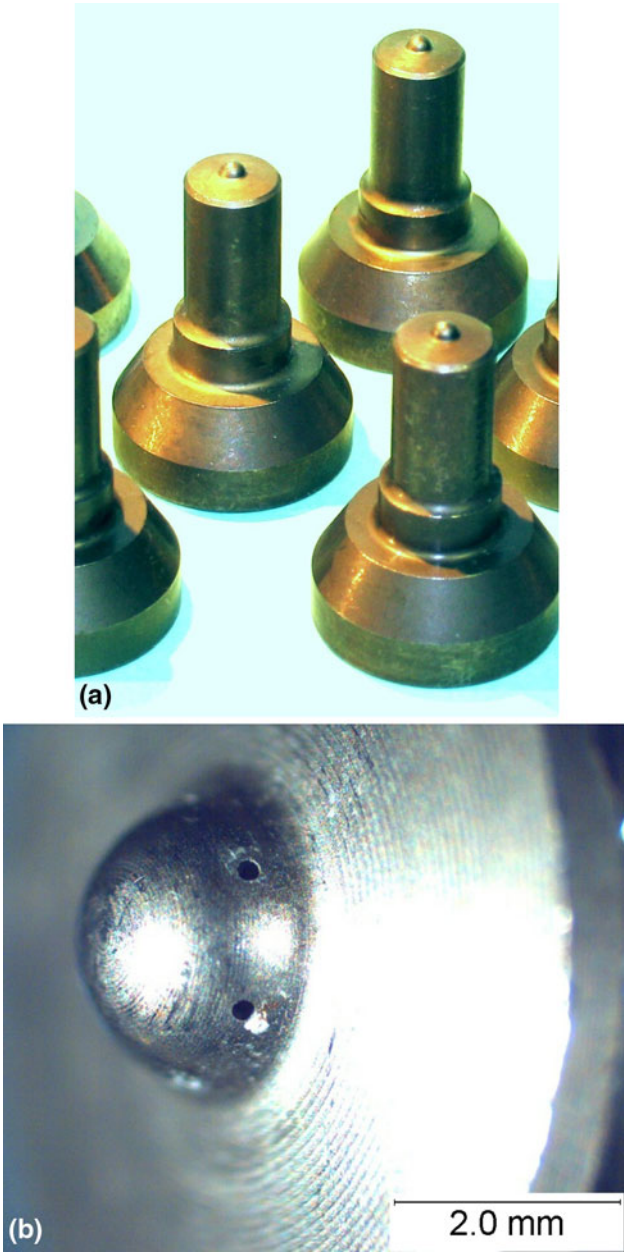

Fig. 1 Fuel injectors of the type characterized here: (a) finished nozzles and (b) close-up of a sack

2.1 Sectioning, Light Optical Metallography, and Hardness Profiles

Nozzles were cross sectioned, polished, and etched with Ralph's etch (25 ml distilled water, 50 ml methyl alcohol, 3 ml HNO_3, 25 ml HCL, 0.5 g copper chloride (II), 1 g ferric chloride (III)) to enable studies of the microstructure in the sack area and to enable characterization of any mechanical property gradients from the inner cavity to the outside surface. Separate studies, not reported here, were conducted to establish that there was a relatively low level of residual compressive stress in the interior of these nozzles; therefore, the microstructures produced during processing and hole-making were expected to most directly influence the properties of the nozzles. Figure 2 shows a deeply etched cross section of a sack (a) and a close-up of the area adjacent to a hole (b). Injector holes show up as

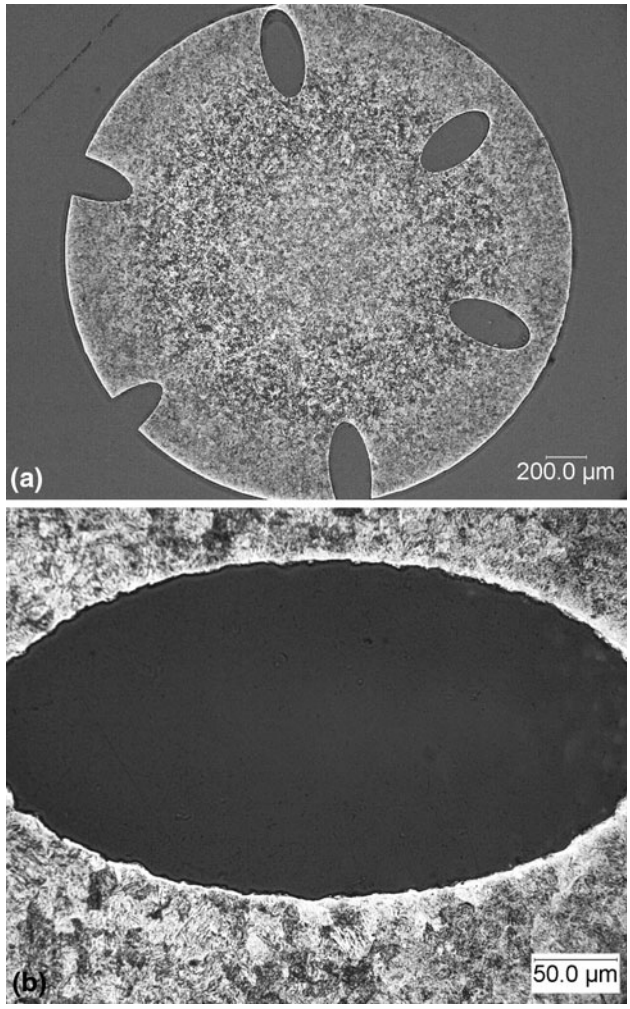

Fig. 2 Etched cross section across the top of a sack showing six spray holes (a), and details of the microstructure surrounding the hole at the upper right (b)

ellipses due to the inclination of the plane of polish relative to the angle in which the six circular holes were produced. Due to the heat treatment given in the nozzle, there was a radial variation in the coarseness of the grain structure of the sack (see Fig. 2a). This variation also corresponded to a variation in microindentation hardness across the tip.

Figure 3 shows the polished, unetched cross section oriented straight across the tip of a sack, parallel to the base. The specimen was sectioned at a location far enough below the top to reveal the central cavity. Figure 4 displays a plot of the Vickers microindentation hardness, HV (103 gf normal force) as a function of distance from the center cavity to the outer surface. Because the section is through a roughly hemispherical tip, the radial distance from the inner cavity to the outside on the plane of polish on the photomicrograph appears larger than the actual wall thickness of the sack. However, the data reveal that the HV at the mid-thickness of the wall, where the grains are coarser, is approximately 25% lower than that of the fine-grained zones nearer the inner and outer surfaces.

2.2 Scanning Electron Microscopy

Using a specially inclined grinding fixture and a series of progressive, precision cuts, it was possible to expose the

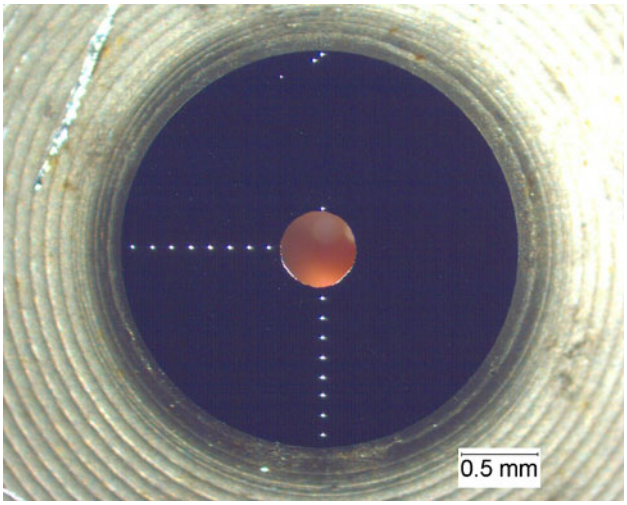

Fig. 3 Polished cross section of a tip showing two HV traces at 90° to one another, from the center to the outside surface

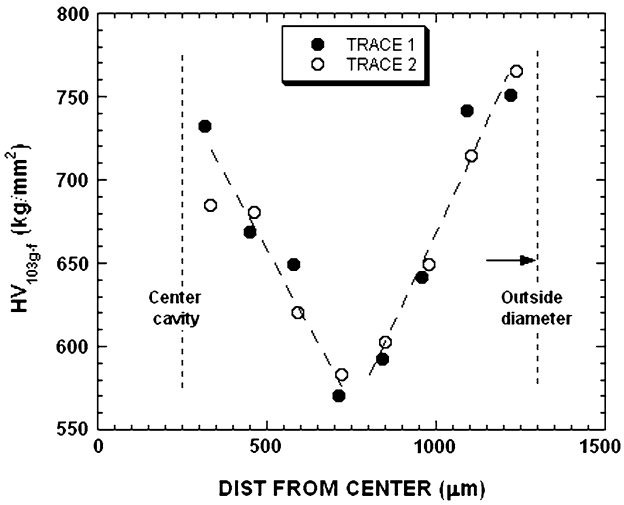

Fig. 4 Variations in HV through the wall of the sack shown in Fig. 3

structure of a single spray hole in the axial direction. Scanning electron microscopy (SEM) was used to study the detailed features of the EDM hole walls, displaying a characteristic splat-like recast layer. Figure 5(a) and (b) shows low and higher magnification images, respectively, of the central portion of the spray hole. The overlapping tongues of metal indicate a relatively rough micro-texture that could affect the flow of the air-fuel mixture through the hole. Individual splats are pocked with cavities and finer-scale protuberances. The fine structure of these features and their thickness variations on the underlying bulk material were revealed by transmission electron microscopy, as described in section 2.4.

SEM was also helpful in revealing the microstructures of the deeply etched cross sections and near-hole regions, like those shown in Fig. 2. Figure 6 shows SEM images of etched regions in the center of the sack wall (a) and the region adjacent to the hole wall. The microstructure of the bulk contains what appears to be a bainitic structure containing regions of acicular carbides. The region near the spray hole (Fig. 6b) shows a loss of granularity and etch-resistant microstructure associated with the

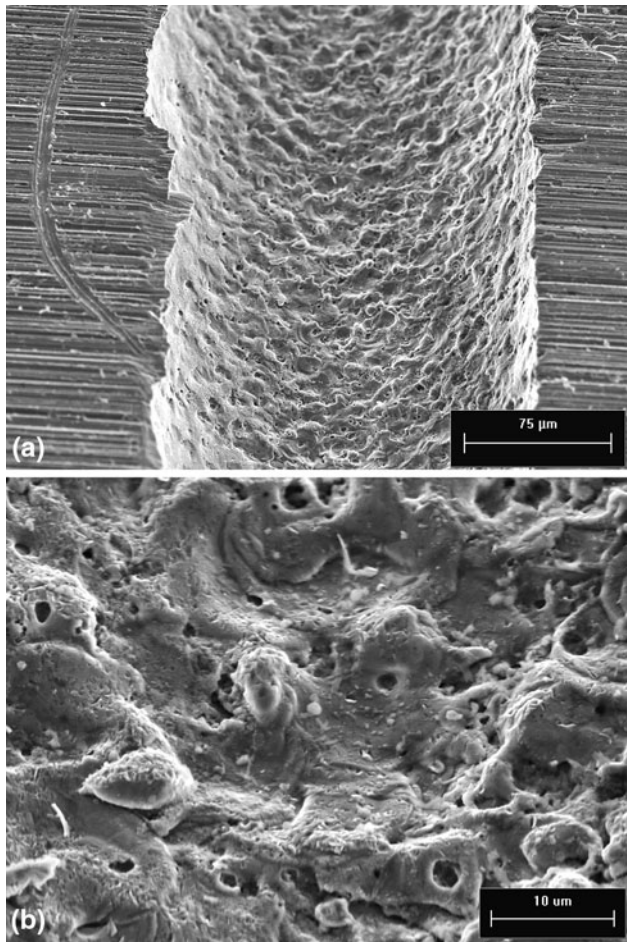

Fig. 5 SEM images of a spray hole wall showing overlapping splat-like features and micrometer-sized pores (Hitachi S3400, variable pressure SEM)

recast layer, here about 0.5-1.0 µm thick. Bars in Fig. 6(b) indicate the location of very fine micro-cracks through recast layer. This suggests that the layer was either extremely fine-grained or mainly amorphous. Transmission electron microscopy, described in section 2.4 supported the former.

2.3 Vertical Scanning Interferometry

Vertical Scanning Interferometry (VSI) is a method of obtaining detailed height maps and measurements of surfaces using the automated counting of optical fringes on a surface as the level of focus is stepped. A general description of VSI methodology and its principle of operation may be found in a recent report by Padula [3]. The current work used a commercial Wyko Model NT9100 instrument to acquire surface maps and measure the roughness variations on the specimen shown in Fig. 5. Two parameters were measured at three locations along the axial direction of the hole: the arithmetic average roughness (Ra) and the ten-point height (Rz), which is the vertical distance between the highest five peaks and lowest five valleys in a sampling length. Data are reported in Table 1. The roughness on the hole wall was as much as half as thick as the recast layer itself. Since the cooling rate of the recast layers during hole-making would be expected to vary with the thickness of the layer and its tortuosity, one might expect a variety of microstructures to be present in that zone, a subject presented in section 2.4.

2.4 Transmission Electron Microscopy

Using the method of focused ion beam (FIB) thinning, it was possible to extract a sliver of material from the centerline of the spray hole wall for cross-sectional study. The plane of the section was taken parallel to the axial direction of the hole to more readily reveal the splat structure of the recast layer using a Hitachi NB-5000 Dual FIB system. The so-called FIB lift-out specimen is a 7×7 μm slice of less than 120 nm in thickness. The FIB specimen was then analyzed using a Hitachi HF-3300 TEM/STEM at 300 kV. Energy-dispersive x-ray spectroscopy (EDS) was carried out to determine the chemical compositions.

Figure 7(a) shows the location on the hole wall where the FIB specimen was taken. Figure 7(b) shows fragments of the recast layer on the hole wall. EDS analysis of these two separate pieces showed they had compositions almost identical to that of the recast layer forming the hole wall. EDS further detected oxygen in the area between the separated recast layer and the surface, suggesting the presence of an oxide. Bright-field TEM image reveals the crystalline (phase) information of a material. Generally, in "Z-contrast" dark-field micrographs, the image contrast increases in proportion to the atomic number (Z) squared. That allows one to discern features such as a precipitate or an oxide scale by its contrast. Nanostructure of the edge of an up-raised portion of the recast layer is revealed in Fig. 8. In this case, the recast layer, having the resemblance of an ocean wave, was more clearly attached to the surface. Elongated grains lay parallel to the free surface of the "wave-front," Fig. 8(a). These elongated grains are less than 30 nm in width exhibit an aspect ratio of well over 6. However, the grains at the opposite face of the wave-front are more equiaxed. Figure 8(b) is a Z-contrast micrograph revealed numerous spherical grains (darker dots of 7 to 20 nm in diameter) near the surface. EDS analysis indicated that these darker spheres are rich in vanadium and chromium. It is likely that high

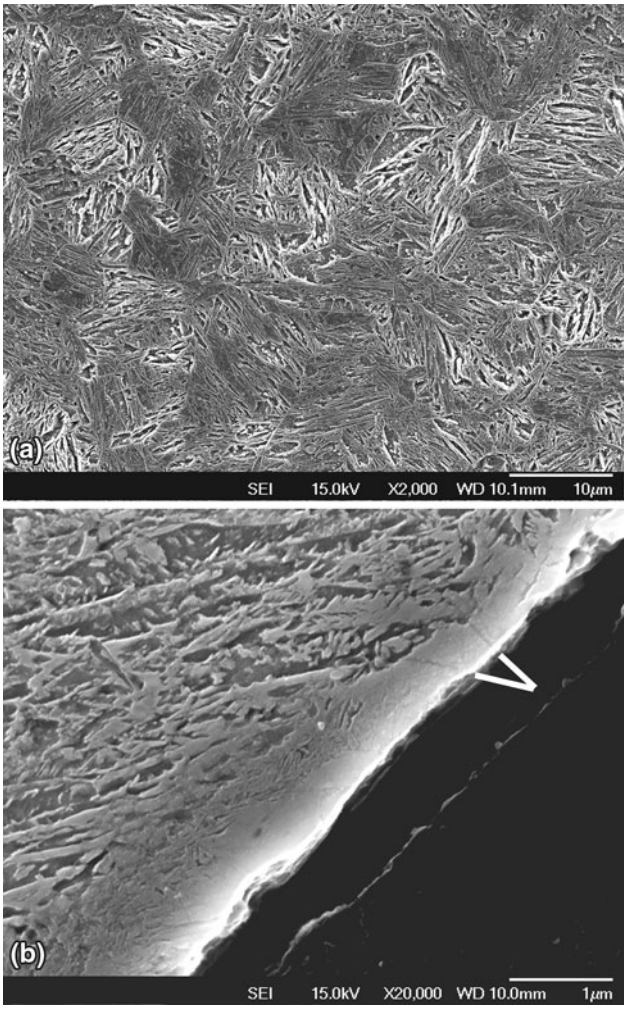

Fig. 6 Ralph's etch reveals a carbide structure within the grains of the sack wall, 0.65 mm from the outside surface (a) and the micro-structure near the wall of a hole (b)

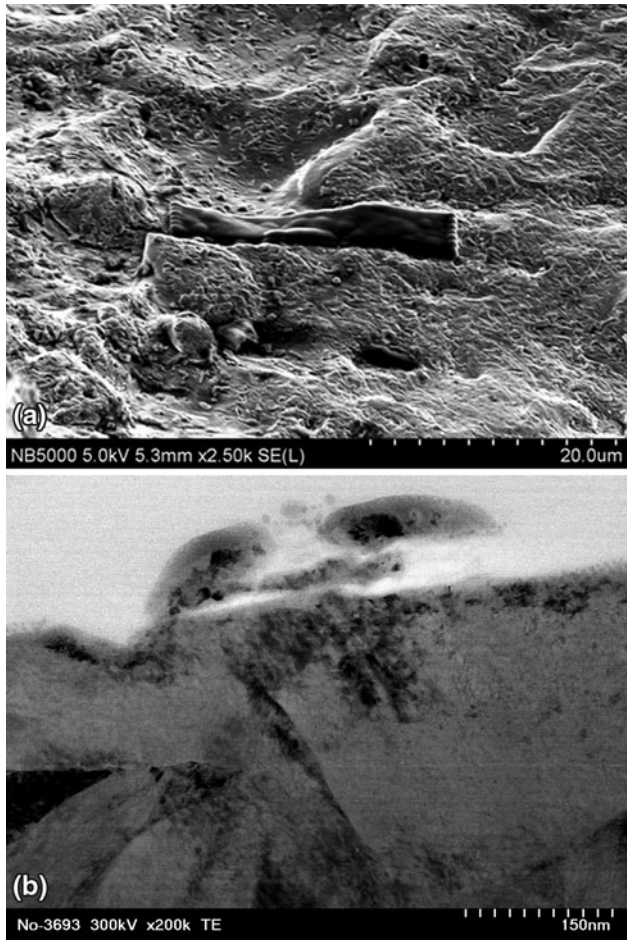

Fig. 7 Preparation and structure of recast layer. (a) Area on the hole wall to be removed by the FIB, (b) bright-field TEM image reveals a recast layer atop the surface and connected by only a very small neck of material

Table 1 Roughness of a spray hole wall

Parameter	Measurement 1, μm	Measurement 2, μm	Measurement 3, μm	Average, μm
Ra	0.61	0.53	0.58	0.57
Rz	3.57	3.31	3.08	3.32

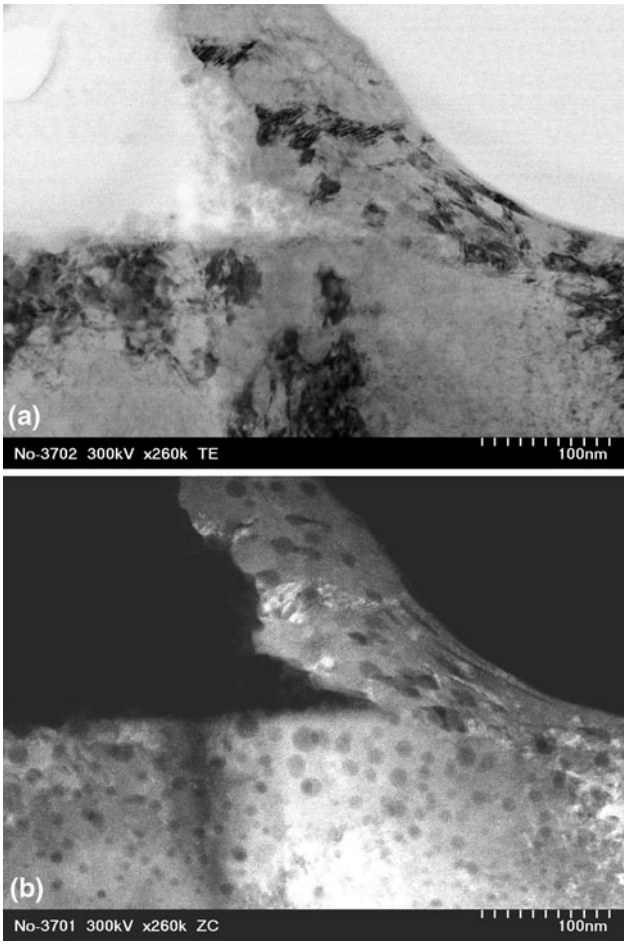

Fig. 8 Nanostructure of the edge of an up-raised portion of the recast layer: (a) bright-field TEM image reveals elongated grains parallel to the surface of the wave; (b) Z-contrast dark-field TEM image showed vanadium- and chromium-rich grains near and at the surface of the alloy

temperature processes caused precipitation of these V- and Cr-rich grains.

In addition to recast layers, the surface was also partially covered by a layer of oxide as shown in Fig. 9. This oxide layer was usually less than 100 nm thick and bonded well with the alloy. In some areas, spherical metal particles were found embedded in this oxide layer.

In summary, the TEM study found that recast layers have varied thickness of up to 200 nm. The recast layers have a wave-like morphology. Some features could have cracks and pores underneath. The recast layers experienced high heat and directional plastic flow. The grains in the recast layer are nanocrystallites, sometimes with flow features. Part of the surface has a layer of oxides of less than 100 nm thick, which contains spherical, cubic particles, richer in Cr than the matrix. The oxide scale is dense and bonds well with the matrix. Spherical particles inside the oxide scales are about 20 nm or less in diameter. The near-surface area of this alloy steel has 50 nm diameter spherical grains, possibly V- or Cr-rich carbides.

2.5 Nanoindentation Hardness Mapping

Nanoindentation studies were conducted using a Hysitron Triboindenter™ to probe the localized gradients in micromechanical properties through the nozzle wall and in the vicinity of the EDM recast layer. The instrument is equipped with a Berkovich Indenter tip (three-sided pyramidal indenter with a 60° apex angle). Prior to testing, the tip was calibrated with a standard fused silica sample to obtain the tip's area function [4]. Every area was tested to 5000 μN load under a constant ramp rate of 500 μN/s. This load produced an average penetration depth of less than 150 nm. The maximum load was maintained for 10 s (hold time) to ensure that the subsequent unloading would be completely elastic. The hardness value for each indentation is calculated from the unloading portion of the curve.

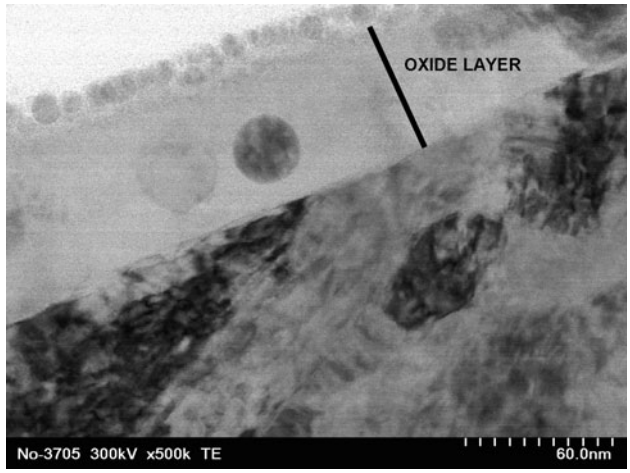

Fig. 9 Oxide layer that partially covers the surface. The spherical grain is an embedded metal particle

The micromechanical properties through the nozzle were obtained from a series of 5 × 5 indentation arrays around the tip sack of the nozzle. Similar to the trend for Vickers microindentation hardness results around the center cavity of the nozzle (see Fig. 4), the hardness at the middle of the sack is approximately 25% lower than the hardness near the surface (Fig. 10a). Further statistical analysis (i.e., ANOVA with $\alpha = 0.5$) indicates that the hardness values can be grouped into different regions (Fig. 10b). The symbols in Fig. 10(b) indicate locations of arrays with the same mean nH number. The mean nH for open circular symbols was not equal to that for any other measured array.

Similarly, the hardness around the vicinity of the EDM recast layer was obtained from a series of 10 indent arrays around the spray hole. Each array started within 1-5 μm from the spray hole edge and continues 135 μm away into the bulk material. The hardness measurements were then grouped and analyzed as a function of distance from the spray hole (Fig. 11a). Additional statistical analysis (i.e., ANOVA with $\alpha = 0.5$) shows no hardness difference from the edge of the spray hole into the bulk on the left, right, and top side. In other words, the EDM re-cast layer does not affect the hardness around the nozzle cavity (within 1 μm from the edge of the spray hole). However, there is a statistical difference in hardness between the top and bottom areas of the spray hole. When the hardness measurements are grouped and analyzed with respect to the nozzle position (i.e., from the edge to the center of the nozzle), the hardness values can be grouped into four different regions, which correlated to the different microstructure found in each area (Figure 11b).

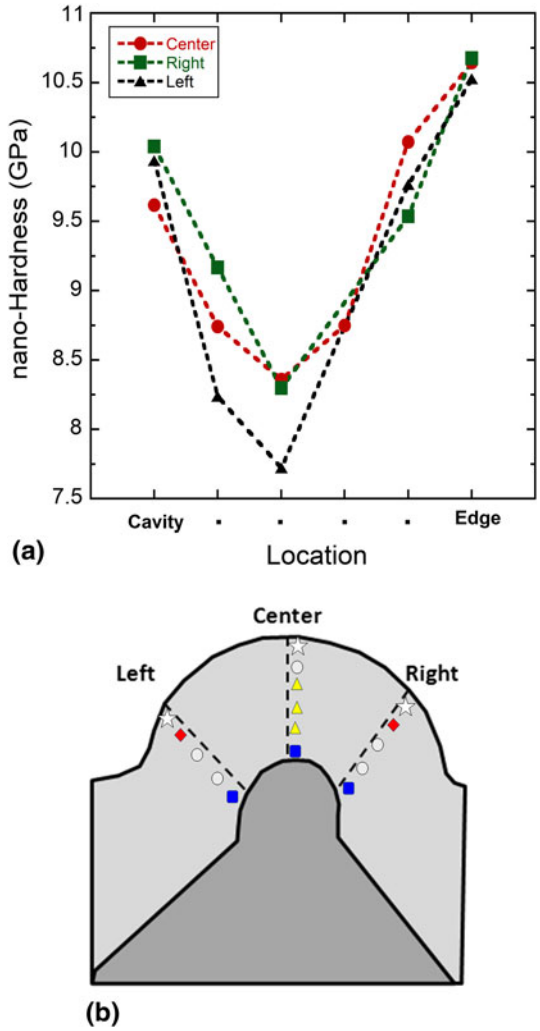

Fig. 10 (a) Average nanoindentation hardness (nH) profiles from the nozzle cavity to the outer edge of the sack. (b) Locations of the three sets of 5×5 indent arrays used to profile nH. The meaning of the symbols is explained in the text

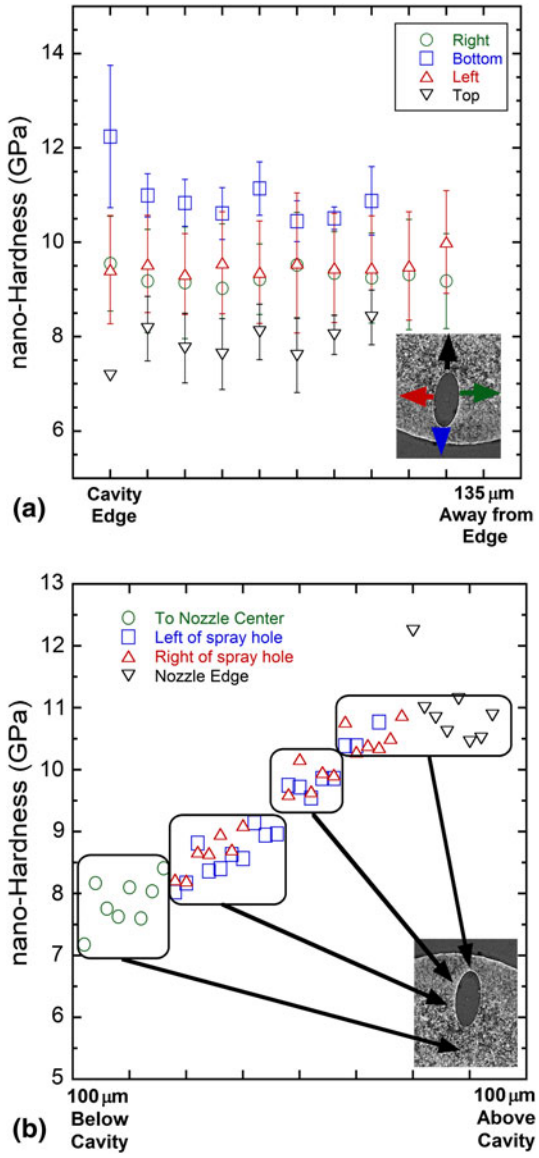

Fig. 11 (a) Average hardness values from the edge of the spray hole into the nozzle bulk. The error bars correspond to one standard deviation. (b) Average hardness values from the edge toward the center of the nozzle. The hardness varies directly proportional to the microstructure (i.e., lower hardness as microstructure grain size increases)

3. Discussion

Several complementary material examination methods provided insights into the nature of the electro-discharge machining hole-making process in terms of how it produced localized changes in the microstructure of an alloy steel. Both microscale and nanoindentation hardness measurements show general trends through the bulk material cross section, but there are less clear results near hole walls. Even though the nanoindentation measurements do not show a statistical difference in hardness near the EDM recast layer, the thinness of the layer fails to allow even these tiny indentations to provide any unambiguous information about its properties. Continuing work on precision sample preparation may expose a larger portion of the re-cast layer and thus allow a better understanding of its properties.

As concerns the potential for EDM holes to initiate fatigue cracks, the fine-scale microstructure, or nanomechanical properties seemed less important than the morphology of the recast layer with its splash-like features, pores, and reentrant surfaces that could serve as stress raisers. Since related studies indicate that low-cycle fatigue crack initiation is more sensitive to surface features than high-cycle fatigue in alloys of this type [5], one might expect that the roughness of EDM hole walls would be more critical in reducing higher-stress, low-cycle fatigue performance than they would lower-stress, high-cycle fatigue performance. Such characterizations will be used to better understand the initiation and propagation of fatigue cracks due to the high cyclical fuel injection pressures designed into current and near-future advanced diesel engines.

4. Summary

Multiple metallographic tools and techniques were employed to gain a better understanding of the microstructure,

nanostructure, and micromechanical properties of electro-discharge-machined (EDM) holes in alloy steel fuel injector nozzle sacks.

- Etching revealed the differences in grain size and the coarsening of the grain structure in the center of the sack walls. It also revealed the non-etching behavior of the sub-micrometer thick recast layers on the hole walls.
- Vickers microindentation hardness of the near-surface areas of sack cross sections was approximately 30% higher than it was at the midpoint of the cross section. This hardness increase corresponds to the finer grain structure revealed by etching, and is likely a result of post-machining heat treatment. Nanoindentation hardness arrays placed in the same areas showed a similar V-shaped hardness profile as microindentation hardness but could not resolve the recast layer hardness near holes.
- The arithmetic average surface roughness of the EDM hole walls was measured using a vertical scanning interferometer, but the numerical values did not reflect the degree of tortuosity evident in the scanning electron microscope and in 3D reconstructions of the hole wall morphology.
- The fine structure of the sub-micrometer thick recast layer was revealed by focused ion beam preparation of a slice of the hole wall for examination in a transmission electron microscope. Spheroidized metallic carbides were observed in the recast layer, but there was no clear difference in nanoindentation hardness in the recast layers despite several attempts to probe this region on polished cross sections through holes.
- The splat-like nature of the recast layer shows numerous areas where cracks could conceivably form under the right stress conditions.

Acknowledgments

This effort was supported in part by the U.S. Department of Energy, Office of Energy Efficiency and Renewable Energy, Office of Vehicle Technologies under a cooperative research and development agreement (CRADA) with Caterpillar Inc. Oak Ridge National Laboratory is managed by UT Battelle LLC under contract to the US Department of Energy. Randy Parten and Tom Geer of ORNL provided valuable help in precision sectioning and metallographic preparation, respectively. The authors wish to thank A. Shyam, ORNL, for his comments during the review.

References

1. R. Morgan, J. Wray, D.A. Kennaird, C. Crua, and M.R. Heikal, *The Influence of Injector Parameters on the Formation and Break-Up of a Diesel Spray*, SAE Paper # 2001-01-0529, Society of Automotive Engineers, Warrendale, PA, 2001, 12 pp
2. U.S. Patents 7,019,247; 6,734,384; 5,951,883; and 5,908,563; held by AA EDM Corporation, Ann Arbor, MI
3. S. Padula II, *Measurement Variability of Vertical Scanning Interferometry Tool Used for Orbiter Window Defect Assessment*, Technical Report NASA/TM-2009-215636, National Aeronautics and Space Administration, Glenn research Center, Cleveland OH, 2009, 15 pp
4. W.C. Oliver and G.M. Pharr, An Improved Technique for Determining Hardness and Elastic Modulus Using Load Displacement Sensing Indentation Experiments, *J. Mater. Res.*, 1992, **7**, p 1564–1583
5. A. Shyam, Materials Science and Technology Division, Oak Ridge National Laboratory, private communication, 2010